



Q-band hyperchromism and B-band hypochromism of bacteriochlorophyll *c* as a tool for investigation of the oligomeric structure of chlorosomes of the green photosynthetic bacterium *Chloroflexus aurantiacus*

Andrei G. Yakovlev¹ · Alexandra S. Taisova¹ · Zoya G. Fetisova¹

Received: 23 September 2019 / Accepted: 31 December 2019 / Published online: 14 January 2020
© Springer Nature B.V. 2020

Abstract

Chlorosomes of green photosynthetic bacteria are the most amazing example of long-range ordered natural light-harvesting antennae. Chlorosomes are the largest among all known photosynthetic light-harvesting structures ($\sim 10^4$ – 10^5 pigments in the aggregated state). The chlorosomal bacteriochlorophyll (BChl) *c/d/e* molecules are organized via self-assembly and do not require proteins to provide a scaffold for efficient light harvesting. Despite numerous investigations, a consensus regarding the spatial structure of chlorosomal antennae has not yet been reached. In the present work, we studied hyperchromism/hypochromism in the chlorosomal BChl *c* Q/B absorption bands of the green photosynthetic bacterium *Chloroflexus* (*Cfx.*) *aurantiacus*. The chlorosomes were isolated from cells grown under different light intensities and therefore, as we discovered earlier, they had different sizes of both BChl *c* antennae and their unit building blocks. We have shown experimentally that the Q-/B-band hyperchromism/hypochromism is proportional to the size of the chlorosomal antenna. We explained theoretically these findings in terms of excitonic intensity borrowing between the Q and B bands for the J-/H-aggregates of the BChls. The theory developed by Gülen (Photosynth Res 87:205–214, 2006) showed the dependence of the Q-/B-band hyperchromism/hypochromism on the structure of the aggregates. For the model of exciton-coupled BChl *c* linear chains within a unit building block, the theory predicted an increase in the hyperchromism/hypochromism with the increase in the number of molecules per chain and a decrease in it with the increase in the number of chains. It was previously shown that this model ensured a good fit with spectroscopy experiments and approximated the BChl *c* low packing density in vivo. The presented experimental and theoretical studies of the Q-/B-band hyperchromism/hypochromism permitted us to conclude that the unit building block of *Cfx. aurantiacus* chlorosomes comprises of several short BChl *c* chains. This conclusion is in accordance with previous linear and nonlinear spectroscopy studies on *Cfx. aurantiacus* chlorosomes.

Keywords Bacterial photosynthesis · Green bacteria · *Chloroflexus aurantiacus* · Chlorosome · Bacteriochlorophyll *c* antenna

Electronic supplementary material The online version of this article (<https://doi.org/10.1007/s11120-019-00707-9>) contains supplementary material, which is available to authorized users.

✉ Andrei G. Yakovlev
yakov@genebee.msu.ru

✉ Zoya G. Fetisova
zfetisova@genebee.msu.ru

¹ Belozersky Institute of Physico-Chemical Biology,
Lomonosov Moscow State University, Leninskie Gory,
Moscow, Russian Federation 119991

Abbreviations

BChl	Bacteriochlorophyll
<i>Cfx</i>	<i>Chloroflexus</i>
CMC	Chlorosome-membrane complexes
<i>Cba</i>	<i>Chlorobaculum</i>
OD	Optical density

Introduction

In green photosynthetic bacteria, chlorosomes are the key light-harvesting extramembrane structures containing $\sim 10^4$ – 10^5 molecules (depending on the species) of

bacteriochlorophyll (BChl) *c/d/e* in the aggregated state (Olson 1998; Pierson and Castenholz 1992, 1995). Chlorosomes have ovoid-shape structures with sizes of ca. 100–260 nm × 40–100 nm × 10–30 nm (Frigaard and Bryant 2006; Oelze and Golecki 1995; Taisova et al. 2002), and are attached to the inner surface of the cytoplasmic membranes. The most amazing property of the chlorosomes is that the BChl *c/d/e* pigments are organized via self-assembly and do not require proteins to provide a scaffold for efficient light harvesting. The self-aggregation of these pigments is due to intrinsic donor–acceptor properties of chlorophylls (Smith et al. 1983; Krasnovsky and Bystrova 1980). The neighboring molecules in the chlorosomal BChl aggregate couple via coordination bonds between the C3¹ hydroxy group and the central Mg atom and via hydrogen bonds between the C13 carbonyl group and the C3¹ hydroxy group. The strong orientational ordering of the BChl *c* Q_y transition dipoles in situ (Fetisova et al. 1988), isolated chlorosome-membrane complexes (Fetisova et al. 1986), and isolated chlorosomes (Mimuro et al. 1994; van Amerongen et al. 1988; van Dorssen et al. 1986) supports the suggestion that the elementary chlorosomal BChl *c* aggregate has the form of a quasi-linear chain.

Besides BChl *c/d/e*, the chlorosomes contain a small amount of BChl *a* (Gerola and Olson 1986) located in the baseplate (Frigaard and Bryant 2006). In *Chloroflexaceae* species, the B798 BChl *a* antenna of the baseplate (Montano et al. 2003) connects the chlorosomal B740 BChl *c* antenna with the membranous B808-866 BChl *a* antenna and reaction centers. The excitation energy transfer within this superantenna occurs according to the cascade scheme: BChl *c* B740 → BChl *a* B798 → BChl *a* B808 → BChl *a* B866 (Martiskainen et al. 2009; van Dorssen and Ames 1988). The BChl *c* B740 → BChl *a* B798 step has a major kinetic component of 10–40 ps depending on the BChl *c* antenna size (Savikhin et al. 1994; Fetisova et al. 1996). All green bacteria are able to grow in a wide range of growth-light intensities due to significant changes of the peripheral BChl *c/d/e* antenna size which is governed by the growth-light intensity (Frigaard and Bryant 2006; Oelze 1992; Pierson and Castenholz 1974; Schmidt et al. 1980; Taisova et al. 2006; Yakovlev et al. 2002b).

Structural models of the BChl *c/d/e* aggregates have been extensively investigated. Many models using a rod-like arrangement of BChl *c/d/e* aggregates were inspired by freeze-fracture electron microscopy data (Egawa et al. 2007; Novoderezhkin et al. 2001; Saga and Tamiaki 2006; Sprague et al. 1981; Staehelin et al. 1978; Yakovlev et al. 2002a). Conversely, a lamellar-type structure for the BChl *c/d/e* aggregates in chlorosomes was proposed in accordance with the X-ray diffraction data (Pšenčík et al. 2004, 2010, 2013). In addition, based on the integration of two different bio-imaging methods, solid-state nuclear magnetic

resonance and cryo-electron microscopy, it was concluded that pairs of alternating *syn-anti*-ligated BChl *c* and *d* stacks form concentric helical nanotubes in chlorosomes from the green sulfur bacterium *Chlorobaculum (Cba) tepidum* mutant (Ganapathy et al. 2009). The combination of several experimental techniques can be useful for quantitative estimation of the curvature variation of the BChl aggregates within the same chlorosomes (Gunther et al. 2016). The validity of these structural models has been examined by comparing various experimental data and theoretical predictions (Arellano et al. 2000; Carbonera et al. 2001; Didraga and Knoster 2003; Dracheva et al. 1998; Fetisova 2004; Fetisova et al. 1986, 1988, 1996; Fetisova and Mairing 1992, 1993; Ganapathy et al. 2009; Gunther et al. 2016; Jendry et al. 2014; Lin et al. 1991; Linnanto and Korppi-Tommola 2008, 2013; Martiskainen et al. 2012; Mairing et al. 1999; Novoderezhkin et al. 1998, 2001; Pšenčík et al. 2010; Savikhin et al. 1998; Sawaya et al. 2015; Shibata et al. 2007; Yakovlev et al. 2002a). Despite the huge amount of research (for review see: Gunther et al. 2016; Fetisova et al. 1988, 1996; Jendry et al. 2014; Mirkovic et al. 2017; Novoderezhkin et al. 2001; Oostergetel et al. 2010; Orf and Blankenship 2013; Pandit and de Groot 2012; Savikhin et al. 1998; Sawaya et al. 2015; Scholes et al. 2011; Yakovlev et al. 2002a), conclusive information on the chlorosomal 3D structure is not yet available. Perhaps, the real structure of the pigment aggregates is a mixture of rod-like and lamellar-like structures (Gunther et al. 2016).

The green nonsulfur thermophilic bacterium, *Chloroflexus (Cfx.) aurantiacus*, is a nice example of filamentous anoxygenic phototrophic bacteria whose peripheral antenna is not very large ($\leq 5 \times 10^4$ BChl *c* molecules, $\sim 2 \times 10^3$ BChl *a* molecules, $\sim 1.5 \times 10^4$ molecules of carotenoids, and $\sim 6 \times 10^3$ molecules of menaquinone-10) (Frigaard and Bryant 2004, 2006). Oligomeric organization of chlorosomal pigments in intact cells of *Cfx. aurantiacus* (as well as in those of *Chlorobium limicola* and *Chlorobium phaeovibrioides*) was proved by the spectral hole-burning method (Fetisova and Mairing 1992, 1993; Fetisova et al. 1994). A long-range molecular order of chlorosomal BChl *c* of *Cfx. aurantiacus* was shown by polarization spectroscopy (Fetisova et al. 1986, 1988; Van Dorssen et al. 1986). The light-controlled variability of the aggregation extent of *Cfx. aurantiacus* peripheral antenna pigments was studied by steady-state and time-resolved spectroscopy (Fetisova et al. 1996; Taisova et al. 2001; Yakovlev et al. 2002b, 2017). The experimental findings were theoretically explained in terms of the tubular model of several exciton-coupled BChl *c* chains within the unit building blocks from which the rod-like structures of BChl *c* aggregates were built in *Cfx. aurantiacus* chlorosomes. Each rod was considered as a sequence of the unit building blocks in accordance with the freeze-fracture electron microscopy data (Fetisova et al. 1996;

Sprague et al. 1981; Staehelin et al. 1978). Optical properties of a tubular aggregate calculated by exciton theory were shown to be dependent on the size of the unit building block and, in particular, on the number of pigments in quasi-linear chains within the unit building block. The number of BChl *c* molecules per each chain within the unit building block was estimated as < 6–7 (Yakovlev et al. 2017). This tubular model was able to explain basic spectroscopic properties of *Cfx. aurantiacus* chlorosomes and approximated the BChl *c* low packing density in chlorosomes in vivo (Fetisova et al. 1996; Taisova et al. 2001; Yakovlev et al. 2002b, 2017).

The green sulfur bacterium *Cba. tepidum* is very attractive due to its extremely large (up to 2.5×10^5 molecules) chlorosomal size (Frigaard and Bryant 2006). Various tubular, lamellar, and rolled lamellar structural models were proposed for *Cba. tepidum* chlorosomes (van Dorssen et al. 1986; Tamiaki 1996; Pšenčík et al. 2004; Furumaki et al. 2011; Linnanto and Korppi-Tommola 2013). To minimize inherent structural heterogeneity of the chlorosomes, the triple mutant (bchQRU) from the species *Cba. tepidum* (Gomez Maqueo Chew et al. 2007) was studied by various techniques (Ganapathy et al. 2009). The structural model of syn-anti stacked dimeric BChl *c* molecules arranged in multilayer tubular superstructures was proposed for this mutant and wild-type *Cba. tepidum* chlorosomes (Ganapathy et al. 2009). Heterogeneous ensemble averaging strongly impeded the study of chlorosomal structure. A study of individual chlorosomes helps to get over this problem in part (Shibata et al. 2006; Furumaki et al. 2011, 2012; Jendryn et al. 2014). A combination of mutagenesis, polarization-resolved single-particle fluorescence excitation spectroscopy, cryo-electron microscopy, and theoretical modeling was used to study the chlorosomal structure of *Cba. tepidum* bchR mutant and to estimate the curvature variation of these aggregates (Günther et al. 2016). Strong intra- and inter-chlorosomal variations of the average curvature of the structural elements were reported. It was concluded that various structural elements (partial cylinders, lamellae, and spirals) can contribute to the structure of chlorosomes during their growth and biogenesis. The structural hierarchy in the pigment organization within an individual chlorosome was shown to be consistent with the multilayer arrangement of BChl aggregates. Thus, the macroscopic ensemble of chlorosomes was characterized by a mixture of organelles with differently curved structures of each individual chlorosome. This may explain the difference in spatial arrangement of the aggregated BChl molecules reported in literature (van Dorssen et al. 1986; Tamiaki 1996; Pšenčík et al. 2004; Linnanto and Korppi-Tommola 2013).

Herein, we studied in detail the phenomena of the Q-band hyperchromism and B-band hypochromism in *Cfx. aurantiacus* chlorosomes isolated from cell cultures grown at different light intensities and therefore having different

size of BChl *c* antennae. Hyperchromism (and its counterpart, hypochromism) is defined as intensity borrowing between the spectral bands. The theory of hyperchromism was originally developed in (Rich and Tinoco 1960; Tinoco 1960, 1962; DeVoe and Tinoco 1962) and then applied to chlorophylls and related molecules by Scherz and Parson (1984a, b). The dependence of the Q_y-band hyperchromism on the antenna size in *Cfx. aurantiacus* chlorosomes was reported earlier (Taisova et al. 2001; Yakovlev et al. 2002b) but this has not been systematically studied. The theory of intensity borrowing between the Soret and Q_y transitions based on the rod-like model of BChl *c/e* aggregates was created for the green sulfur bacteria *Chlorobium phaeobacteroides* and *Chlorobium tepidum* (Shibata et al. 2010). A simple theory of excitonic intensity borrowing between the Q and B bands for J-/H-aggregates of the BChls was developed by Gülen (2006). This theory showed the dependence of the Q-/B-band hyperchromism/hypochromism on the structure of the aggregates. For example, for the model of exciton-coupled BChl *c* linear chains, this theory predicted the dependence of the hyperchromism on the number of molecules per chain and the number of chains. In the present work, we showed experimentally an increase in the Q-/B-band hyperchromism/hypochromism with increasing in the antenna size and explained this fact by an increase in the number of BChl *c* molecules per chain in accordance with the theory of Gülen (2006). A comparison of our experimental data and this theory led to conclusion that the unit building block of *Cfx. aurantiacus* chlorosomes contains several short BChl *c* chains. This conclusion is consistent with our previous linear and nonlinear spectroscopy studies on *Cfx. aurantiacus* chlorosomes (Fetisova et al. 1996; Yakovlev et al. 2002b, 2017).

Materials and methods

Growth

Cells of filamentous thermophilic green bacterium *Chloroflexus aurantiacus* strain Ok-70-fl (collection of Leiden University, The Netherlands) were cultivated anaerobically in batch cultures with constant stirring at 55 °C on a standard medium (Pierson and Castenholz 1974; Castenholz 1969, Supplement) at different light intensities from incandescent lamps. The emission spectrum of the lamps is presented in Supplement. Different light intensities were achieved by varying the number of lamps, the light power of each lamp, and the distance from the light source. The corresponding incident photon flux density was varied from ~ 3 to ~ 60 $\mu\text{E m}^{-2} \text{s}^{-1}$.

Isolation of chlorosome-membrane complexes

Chlorosome-membrane complexes (CMC) were isolated from *Cfx. aurantiacus* cell cultures grown at different light intensities. Consequently, these CMC had different BChl *c* contents. CMC were prepared from fresh *Cfx. aurantiacus* cells by the method of Ma et al. (1996) in slight modification. Fresh cells were harvested by centrifugation at 8500×*g* for 20 min, washed with 10 mM Tris–HCl buffer, pH 8.0 and suspended in TA buffer (10 mM Tris–HCl buffer pH 8.0 containing 10 mM sodium ascorbate). The suspension was disrupted by two passes through a French pressure cell at 20,000 psi in the presence of 2 mM phenylmethylsulfonyl fluoride. Unbroken cell and large debris were removed by centrifugation at 20,000×*g* for 30 min at 4° C. The supernatant was centrifugated for 90 min at 180,000×*g* (45,000 rpm, Ti 50) at 4° C, and the resulting pellet was resuspended in a small volume of TA buffer, and diluted with 0.7 vol. of glycerol before storing at –70 °C. It contained the cytoplasmic membranes with attached chlorosomes.

Chlorosome isolation

Chlorosomes were isolated from *Cfx. aurantiacus* CMC suspension in TA buffer in a twofold successive continuous sucrose gradient (55–20% (wt/wt) and 45–15% (wt/wt) as described earlier in modification for CMC (Taisova et al. 2002). Continuous sucrose density gradients were prepared in 50 mM Tris–HCl buffer, pH 8.0, and 2 M NaSCN (Tris-thiocyanate buffer) in the presence of 10 mM sodium ascorbate in centrifuge tubes each containing a total of 38 ml. 1.5–2.0 ml of the CMC suspension with optical density 150–170 optical units at 740 nm was carefully added on top of each sucrose gradient. After centrifugation for 20 h at 135,000×*g* (28 000 rpm, SW-28) at 4° C, the chlorosomes banding between 28 and 30% sucrose were collected (based on the amplitude of absorption at ~740 nm).

Spectroscopy

Ground state absorption spectra of chlorosomes were recorded at room temperature with a Hitachi-557 spectrophotometer (Japan). We used only freshly isolated samples of chlorosomes in all measurements.

Results

Figure 1 shows the absorption spectra of *Cfx. aurantiacus* chlorosomes isolated from cells grown under different light intensities and diluted into aqueous.

Tris buffer and into the equivalent amount of acetone-methanol mixture, 7:2. Thus, the material concentrations

in the pairs of samples in Fig. 1 were the same. The spectra of chlorosomes in Tris buffer consisted of a well-separated Q_y band (13,514 cm⁻¹ or 740 nm) and a broad Soret (B) band (maximum at 21,834 cm⁻¹ or 458 nm) of BChl *c* aggregates. A very small band at 12,580 cm⁻¹ (795 nm) belonged to the baseplate BChl *a*. The broad, shapeless tail of the Q_y band (15,000–18,000 cm⁻¹) probably contained a weak Q_x band and higher-energy Q transitions. Carotenoids mainly contributed to the region between 18,000 and 20,500 cm⁻¹ in Tris buffer spectra. The Soret band comprised of a strongly overlapping unresolved mixture of B_x and B_y bands. Theoretical modeling of the optical spectra of the BChl *c* aggregates showed that the contributions of both bands to the Soret band were comparable, but the energy of the B_y transition was somewhat less than that of the B_x transition (Shibata et al. 2010).

Dilution in a polar solvent (acetone) led to the monomerization of BChl *c* aggregates (Clayton 1980) which clearly caused noticeable changes in the absorption spectra (Fig. 1, blue). The monomeric Q_y- and B-bands of BChl *c* are shifted to ~15,133 cm⁻¹ (661 nm) and ~23,234 cm⁻¹ (430 nm), respectively. A small band at ~16,000 cm⁻¹ (625 nm) probably belongs to a mixture of the monomeric Q_x band and the higher-energy Q_y-vibrational transition of BChl *c*. The two peaks at ~20,600 and 21,800 cm⁻¹ (485 and 460 nm) in acetone-methanol spectra belong to carotenoids. For comparison, pure BChl *c* dissolved in acetone has major absorption peaks at 15,150 (Q_y) and 23,100 (B) cm⁻¹ and minor peaks at 16,000 (Q), 24,250 (B), and 25,600 (B) cm⁻¹ (Shibata et al. 2010). Quantum chemical calculation of the Chl *a* (a closest relative to BChl *c*) absorption spectrum revealed ~10 transitions in the B band in addition to two transitions in the Q band (Q_x and Q_y) (Graczyk et al. 2014). The spectra of chlorosomes from the cells grown under different light intensities and extracted with acetone-methanol mixture were not the same (Fig. 1) due to different ratios of pigments. For example, chlorosomes from the low-light-grown cells (Fig. 1d) contained less carotenoids per BChl than chlorosomes from the high-light-grown cells (Fig. 1a).

It is clearly seen in Fig. 1 that the oligomerization of chlorosomal BChl *c* led to an enhancement of the Q_y band and a reduction of the B band due to B → Q intensity borrowing. The B-band reduction mainly occurred near the B-band maximum. To characterize this phenomenon quantitatively, we introduced the term hyperchromism *H* as the relative difference between the areas under spectral curves of the chlorosomal (*S*_{Q,B}) and monomeric (*S*_{Q,B}⁰) BChl *c* bands:

$$H_{Q,B} = (S_{Q,B} - S_{Q,B}^0) / S_{Q,B}^0 = S_{Q,B} / S_{Q,B}^0 - 1 \quad (1)$$

A positive/negative *H* value corresponds to hyperchromism/hypochromism.

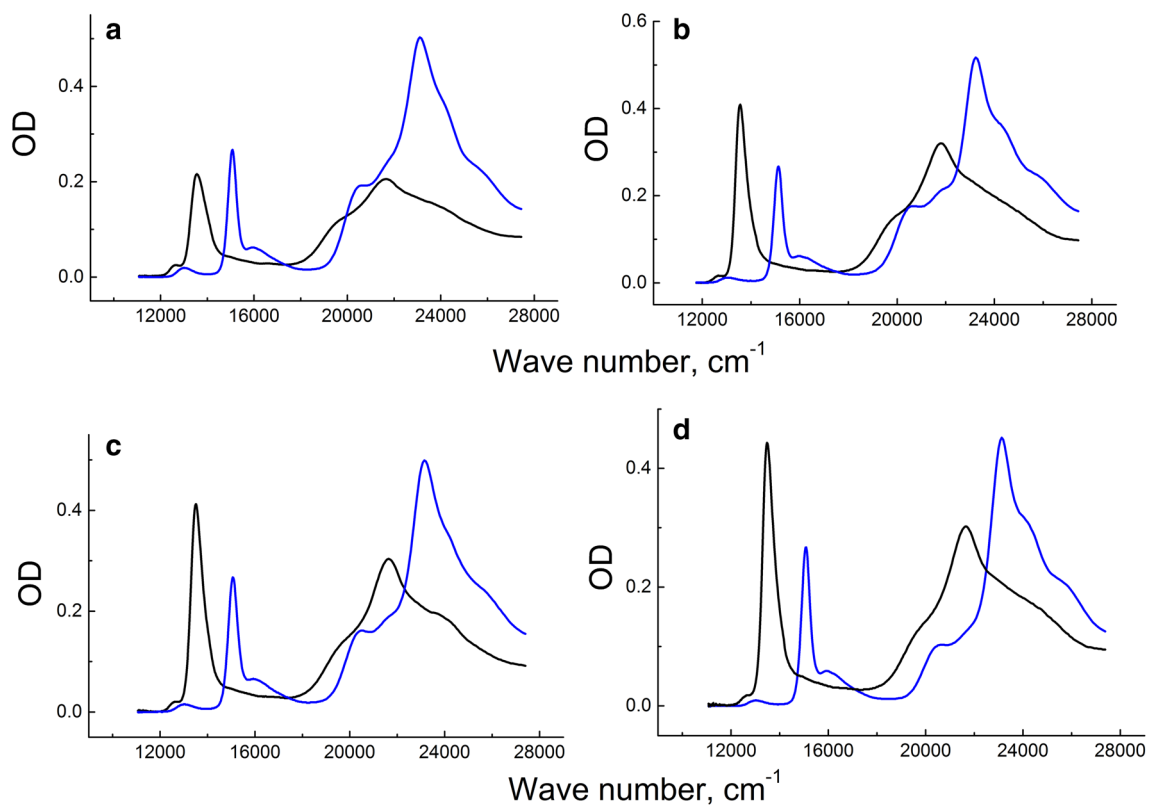


Fig. 1 The absorption spectra of *Cfx. aurantiacus* chlorosomes isolated from cells grown under light intensities of 1 (**d**), 3 (**c**), 10 (**b**), and 20 (**a**) relative units, diluted into aqueous Tris buffer (black) and into the equivalent amount of acetone-methanol, 7:2 (blue)

The main problem in calculating $S_{Q,B}$ and $S_{Q,B}^0$ is the uncertainty in the integration limits due to very complicated shape of the multi-band absorption spectrum of *Cfx. aurantiacus* chlorosomes. It is almost impossible to separate strongly mixed B_y and B_x bands. Also, it is difficult to define correctly the high-energy limit of the Q_y band. To simplify the task, we separated the spectral contributions of carotenoids and BChl *a* from those of BChl *c* in Tris buffer and acetone-methanol spectra of chlorosomes. For this, we fitted the spectral bands of carotenoids and BChl *a* with Gaussian profiles and subtracted them from the original spectra of chlorosomes. The spectra of carotenoids were fitted with two Gaussian profiles, and the spectrum of BChl *a* was fitted with single Gaussian profile. Parameters of the fitting corresponded to the complete absence of the spectral bands of carotenoids and BChl *a* in the residual spectra. Thus, the residual spectra that remained after subtraction mainly contained the $Q_{x,y}$ and $B_{x,y}$ bands of BChl *c*. We did not use the fitting procedure for separation of the “x” and “y” bands because of their evident overlap and possible mixing and interaction between them. The residual spectra were used for further calculations. We synchronously varied the integration limits of $S_{Q,B}$ and $S_{Q,B}^0$ in the same proportions to minimize the corresponding error. We

started from narrow limits of integration included only the main Q_y peak and the central part of the B band and gradually increased them up to the whole Q and B bands. Thus, the integration limits were changed approximately from 12,000–14,600 to 12,000–17,500 cm^{-1} (Q band, Tris buffer), from 19,500–23,500 to 17,500–27,500 cm^{-1} (B band, Tris buffer), from 14,000–16,000 to 14,000–18,500 cm^{-1} (Q band, acetone-methanol), and from 22,000–24,000 to 20,000–27,500 cm^{-1} (B band, acetone-methanol). The upper limit of B-band integration (27,500 cm^{-1}) was just the limit of the spectrometer. These different calculations produced a spread of calculated H values (see Fig. 2). A minimal and maximal H for each experimental point corresponded to underestimated and overestimated values of H , respectively. It should be noticed that the applied method of calculation did not provide a full guarantee of correct extracting of the Q_y and B bands from the measured spectra, and therefore it could be used for the approximate estimation of the H values.

Figure 2 shows the dependence of the Q_y -band hyperchromism and the B-band hypochromism of *Cfx. aurantiacus* chlorosomes on the light intensity used for bacterial growth. An increase in the light intensity led to a decrease in both the Q_y -band hyperchromism and the B-band hypochromism.

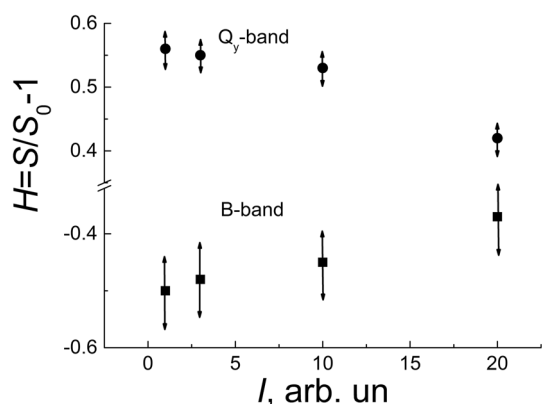


Fig. 2 The dependence of the Q_y -band hyperchromism and the B-band hypochromism of *Cfx. aurantiacus* chlorosomes on the light intensity used for bacterial growth. Double arrows show the scatter of points due to variation of the integration limits in the calculations of S and S_0

The absolute values of the positive Q_y -band hyperchromism and the negative B-band hypochromism were close one to another. The spread of H values (shown by double arrows in Fig. 2) reflects an uncertainty in the integration limits in the calculation of $S_{Q,B}$ and $S_{Q,B}^0$. The corresponding error was moderate in the case of integration of the Q_y spectrum, but large for the B spectrum. Formally, the large spread for the B-band data points permitted to draw even a horizontal $H(I)$ line, but the lower and upper H values for each I clearly showed that H depends on I .

It is known that a change in the light intensity used for bacterial growth led to a change in the chlorosomal antenna size (Fetisova et al. 1996; Taisova et al. 2001; Yakovlev et al. 2002b, 2017). To relate the experimental values of the light intensity used for the growth of *Cfx. aurantiacus* cultures to the chlorosomal antenna sizes in these cultures, we measured the absorption spectra of *Cfx. aurantiacus* CMC grown at different light intensities (Fig. 3). The maximum of spectra at $13,514 \text{ cm}^{-1}$ (740 nm) belonged to chlorosomal BChl c , while the maxima at $12,376$ and $11,547 \text{ cm}^{-1}$ (808 and 866 nm) belonged to the membrane core BChl a antenna B808–866. It is known that the size of the core B808–866 antenna does not depend on the growth-light conditions (Olson 1980; Golecki and Oelze 1987). Based on this fact, we normalized the CMC absorption spectra at $11,547 \text{ cm}^{-1}$ and characterized the different BChl c contents in chlorosomes according to the ratios of absorption peaks at $13,514$ and $11,547 \text{ cm}^{-1}$. Consequently, a 20-fold increase in the light intensity during the cell culturing resulted in a ~ 3.5 -fold increase in the content of the chlorosomal BChl c in our experiment. Figure 4 shows the dependence of the Q_y -band hyperchromism and the B-band hypochromism on the ratio of *Cfx. aurantiacus* cells absorption at 740 and 866 nm.

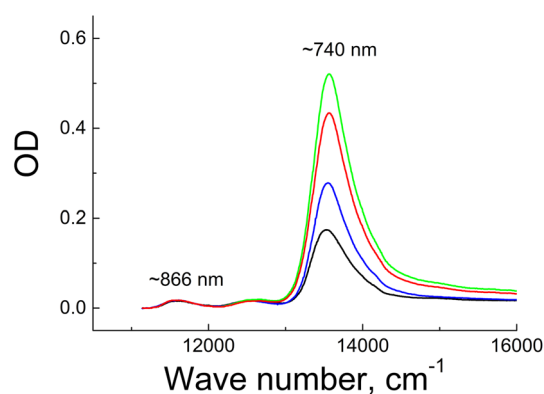


Fig. 3 The absorption spectra of chlorosome-membrane complexes isolated from *Cfx. aurantiacus* cell cultures, grown at light intensity of 20 (black), 10 (blue), 3 (red), and 1 (green) relative units. The spectra are normalized to the absorption maximum of the core B808–B866 antenna at 866 nm since its size does not depend on the growth-light conditions

Both hyper- and hypochromism increased with increasing in the chlorosomal antenna size, but the rate of these changes (the first derivative of $dH/d(\text{antenna size})$) gradually decreased. It is clear that an increase in the chlorosomal antenna size itself cannot change the intensity of borrowing between the BChl spectral bands. The observed changes in hyper(hypo)chromism unambiguously indicate some structural variation in the chlorosomal antenna.

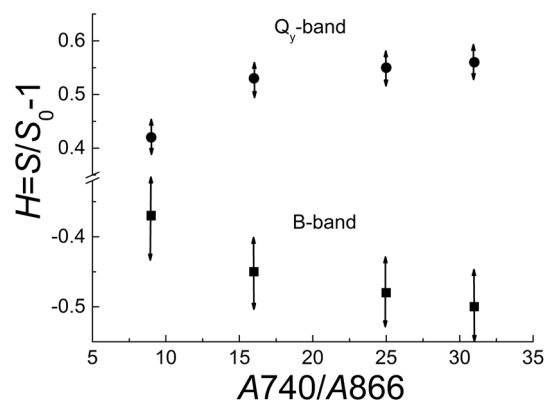


Fig. 4 The dependence of the Q_y -band hyperchromism and the B-band hypochromism on the ratio of *Cfx. aurantiacus* absorption at 740 and 866 nm (see Fig. 3). Double arrows show the scatter of points due to variation of the integration limits in the calculations of S and S_0

Discussion

Model of Q/B hyperchromism/hypochromism

To explain the obtained data, we addressed to the theory of B–Q intensity borrowing in the J-/H-aggregates of BChls (Gülen 2006). The terms “J-/H-aggregates” denote the “nose to tail” and “nose to nose” spatial arrangement of transition dipole moments, respectively. This theory is based on the following approaches and assumptions: the point dipole approximation, the nearest neighbor interaction, homogeneous aggregates, the same polarization of the Q and B transitions, and consideration of the excited states only. It is clear that a set of these assumptions prevent a detailed quantitative explanation of our experiment. The most important drawback of the theory is the point dipole approximation which is not valid in tightly packed BChl aggregates. To our knowledge, an adequate theory of the hyper(hypo)chromism in *Cfx. aurantiacus* is not available now. By these reasons, we used the theory of Gülen for illustrative purpose for a general explanation of the basic effects. The validity of applying this theory to *Cfx. aurantiacus* chlorosomes is discussed below. A general conclusion made in (Gülen 2006) is that the Q–B interband mixing is mediated by the coupling between the excitonic transitions in the Q and B spectral bands. Consequently, the Q–B band mixing significantly affected the spectral properties of these bands. The spatial structure of molecular aggregates is assumed to be constructed from parallel chains of molecules. The main parameters used in (Gülen 2006) were the energies and dipole moments of monomeric Q and B transitions, intraband (Q–Q and B–B) and interband (B–Q) couplings, the number of molecules per chain, and the number of chains. The last two parameters referred to the spatial structure of molecular aggregates.

To check the validity of the model used, we calculated spectra of the Q_y and B_y absorption bands of *Cfx. aurantiacus* chlorosomes and of the monomeric BChl *c* bands (Fig. 5). For realism, a mixture of aggregates with $N=2$, 3, and 4 molecules (with relative contribution of 0.3:1:2, respectively) per chain and the Gaussian shape of each exciton band were assumed for the chlorosomal spectra. Most features of the calculated spectra such as the Q-band hyperchromism, B-band hypochromism, red shift of the chlorosomal spectra compared to the spectra of monomeric BChl *c*, and the high-energy tail of the chlorosomal bands are in accordance with those of the experimental spectra. The calculated difference in the amplitudes of chlorosomal and monomeric bands, the energies of the Q_y and B_y bands, and their bandwidths are in accordance with the experimental ones, while the shapes of the calculated and

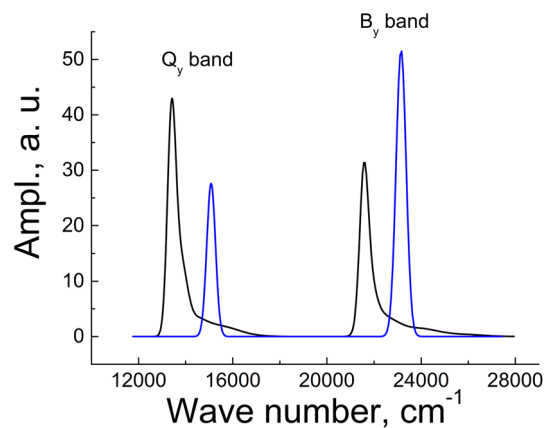


Fig. 5 The calculated spectra of the Q_y and B_y absorption bands of *Cfx. aurantiacus* chlorosomes (black) and the bands of monomeric BChl *c* (blue). A mixture of aggregates with $N=2$, 3, and 4 molecules (with relative contribution of 0.3:1:2, respectively) per chain in a 6-chain tube was assumed. The Gaussian shape of each exciton band with FWHM=250 and 300 cm^{-1} was assumed for the Q_y and B_y bands, respectively. Parameters of the calculation were as follows: energy of the monomeric Q_y transition $E_Q=15,075 \text{ cm}^{-1}$, energy of the monomeric B_y transition $E_B=23,125 \text{ cm}^{-1}$, the Q_y - Q_y coupling $V_{QQ}=-970 \text{ cm}^{-1}$, interchain Q_y - Q_y coupling $V'_{QQ}=49 \text{ cm}^{-1}$, the number of chains $L=6$, and the ratio of dipole moments of B_y and Q_y transitions $\mu_B/\mu_Q=1.38$. Note that the B-B and B-Q couplings can be scaled as $V_{BB}=(\mu_B/\mu_Q)^2V_{QQ}$ and $V_{BQ}=(\mu_B/\mu_Q)V_{QQ}$

experimental bands are not similar (see Fig. 1 for comparison). The deviation in the calculated shape of the Q band from the experimental one is moderate, but this deviation is much more evident for the B band. It is clear that taking into account the Q_x and B_x transitions would improve the used approach. Figure 6 shows theoretical dependence of the Q_y and B_y absorption strengths and peaks on the number of molecules, N , per chain. A proportional increase in the strengths and a small red shift of the bands with increase in N is in accordance with the previously reported results (Yakovlev et al. 2017). One can conclude that the theory of Gülen (2006) can be used for qualitative explanation of the hyper(hypo) chromism in *Cfx. aurantiacus* chlorosomes, but more rigorous theory is needed to adequately describe interactions between aggregated molecules in *Cfx. aurantiacus* chlorosomes.

Figure 7 shows the theoretical dependences of the Q-band hyperchromism and of the B-band hypochromism on the number of molecules per chain, N , for the 6-chain aggregate. For realism, we used fractional N to imitate a mixture of aggregates with different N . The monomeric transition energies of 15,075 and 23,125 cm^{-1} were taken at the peaks of experimental Q_y and B absorption bands (Fig. 1). The ratio of the dipole moments of the monomeric Q and B transitions was taken as $\mu_B/\mu_Q=1.38$ that is in the range of estimations (Scherz and Parson 1984a, b; Umetsu et al. 1999). The Q–Q coupling V_{QQ} was taken

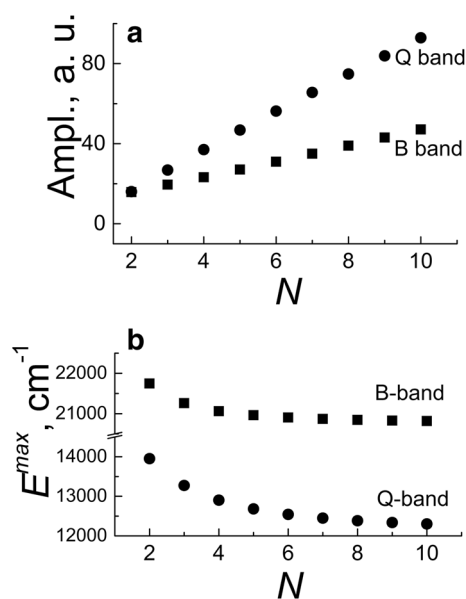


Fig. 6 Theoretical dependence of the Q_y and B_y absorption strengths (see Fig. 5) (a) and their peak energy (b) on the number of molecules per chain N . See the legends in Fig. 5 for other parameters

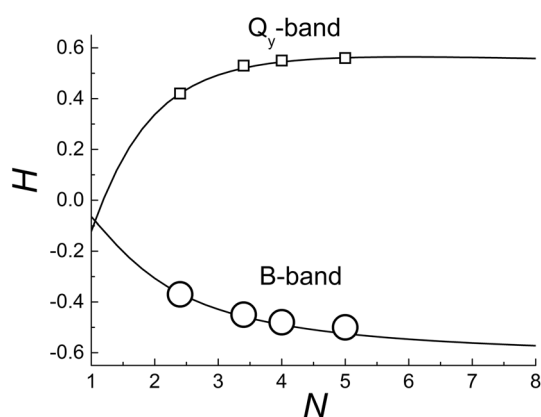


Fig. 7 Experimental (squares and circles) and theoretical (solid curves) dependences of the Q_y -band hyperchromism and the B-band hypochromism of *Cfx. aurantiacus* chlorosomes on the number N of BChl c molecules per chain. Fractional N was used to imitate a mixture of chlorosomes with different N . The size of the experimental points reflects the spread in the H values. See the legend in Fig. 5 for other parameters

as -970 cm^{-1} that agreed with close proximity of the self-aggregated BChls (Pšenčík et al. 2004; Umetsu et al. 1999; Tamiaki et al. 2002). The coupling between chains was taken as 49 cm^{-1} that is close to the value used in previous theoretical simulations of linear and nonlinear spectra of tubular BChl c aggregates (Mauring et al. 1999; Yakovlev et al. 2017). The number of chains $L=6$ was taken as in (Mauring et al. 1999; Yakovlev et al. 2017).

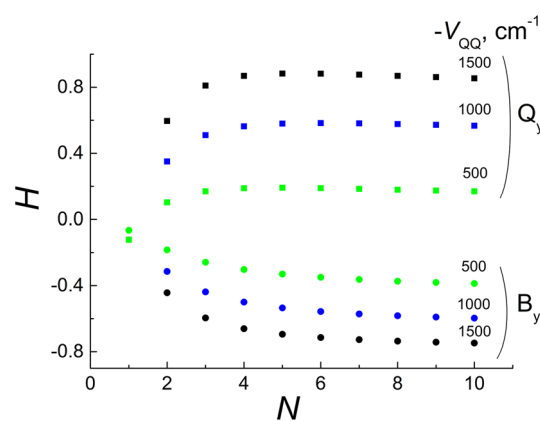


Fig. 8 Theoretical dependence of the Q_y -band hyperchromism and the B_y -band hypochromism on the number of molecules per chain N for different values of the Q-Q coupling $V_{QQ} = -1500, -1000$, and -500 cm^{-1} . See the legend in Fig. 5 for other parameters

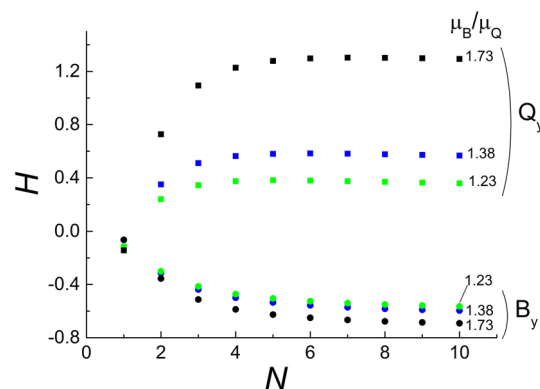


Fig. 9 Theoretical dependence of the Q_y -band hyperchromism and the B_y -band hypochromism on the number of molecules per chain N for different values of the ratio of the dipole moments of B_y and Q_y transitions $\mu_B/\mu_Q = 1.73, 1.38$, and 1.23 . See the legend in Fig. 5 for other parameters

The theoretical curves in Fig. 7 show an increase in both Q-band hyperchromism and B-band hypochromism with increase in N . This increase is conspicuous for a small $N=1-3$ but much less for $N>5$. We arbitrarily put the experimental points on the theoretical curves in Fig. 7. Notice that we could not know the N values for each point and therefore used the relative difference of their H values. The experimental points are in close accordance with the theoretical curves if we assume a mixture of aggregates with different N in the experiment. For example, two experimental points with $N=2.4$ and $N=3.4$ can be considered as a mixture of $N=2/N=3$ and $N=3/N=4$ aggregates in a ratio of 3:2, respectively. The main conclusion from Fig. 5 is that BChl c aggregates of *Cfx. aurantiacus* chlorosomes can be built from the units with the short molecular chains.

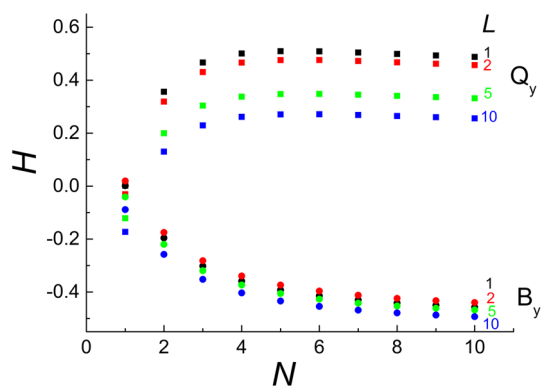


Fig. 10 Theoretical dependence of the Q_y-band hyperchromism and the B_y-band hypochromism on the number of molecules per chain *N* for the different number of chains *L* = 1, 2, 5, and 10. See the legend in Fig. 5 for other parameters

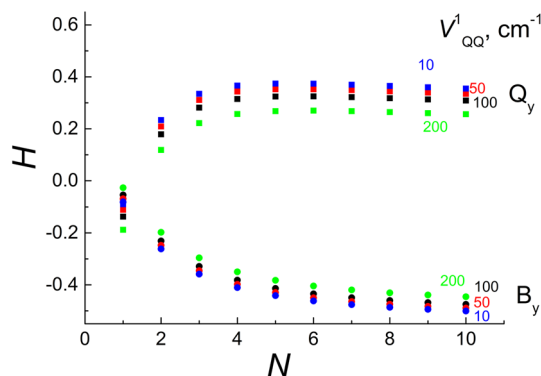


Fig. 11 Theoretical dependence of the Q_y-band hyperchromism and the B_y-band hypochromism on the number of molecules per chain *N* for different values of the interchain coupling $V^1_{QQ} = 10, 50, 100,$ and 200 cm^{-1} . See the legend in Fig. 5 for other parameters

Variation of theoretical parameters over a wide range did not change this conclusion (Figs. 8, 9, 10, 11). This variation changed the *H* values in the Q- and B-bands, but the qualitative character of the *H(N)* dependences remained the same. For example, an increase in the Q–Q coupling V_{QQ} from -500 to -1500 cm^{-1} and an increase in the μ_B/μ_Q ratio from 1.22 to 1.73 led to a conspicuous increase in *H* (more pronounced in the Q band than in the B-band) (Figs. 8 and 9). An increase in the number of chains *L* from 1 to 10 resulted in a decrease in the Q-band hyperchromism and a small increase in the B-band hypochromism (Fig. 10). An increase in the interchain coupling V^1_{QQ} from 10 to 200 cm^{-1} led to a decrease in both Q-band hyperchromism and B-band hypochromism (Fig. 11). All of the *H(N)* dependences shown in Figs. 6, 7, 8 and 9, are qualitatively similar: the region of conspicuous increase at $N = 1-4$ is followed by the region of much smaller changes at $N > 5-6$. It should be noted that $N = 1$ corresponded to the ring of *L* molecules in

the calculations, therefore $H(N = 1, L)$ is equal to zero (as it should be for monomers) only if $L = 1$ (see Fig. 10). Based on Fig. 7, we estimated the BChl *c* content for the building units of chlorosomes grown at high- and low-light intensity as $2.4 \times 6 \sim 14$ and $5 \times 6 = 30$ molecules per unit, respectively. These estimations accorded with previously obtained ones which were based on the tubular-model calculations of the steady-state and time-resolved spectra of *Cfx. aurantiacus* chlorosomes (Yakovlev et al. 2017).

Discussion on the chlorosome structure

In further discussion, we addressed to the available information on the in vivo BChl *c* packing density for *Cfx. aurantiacus* chlorosomes (Staehelin et al. 1978; Golecki and Oelze 1987; Sprague et al. 1981). This information, together with its analysis, is summarized in Table 1.

According to freeze-fracture electron microscopy, *Cfx. aurantiacus* chlorosomes with low/high BChl *c* content had an average height of 12/19 nm, a width of 34/38 nm, and a length of 96/108 nm. The chlorosomes contained $\sim 3400/12,000$ molecules collected in $\sim 12/21$ rods, each ~ 5.5 nm in diameter. Thus, each rod contained $\sim 280/570$ molecules. Electron microscopy revealed a 6-nm periodicity in the rod structure (Staehelin et al. 1978; Sprague et al. 1981). Assuming that each rod consisted of 6-nm units, we calculated the number of units per rod as 16/18, and the number of molecules per unit as 18/32. Assuming further that each unit consisted of 6 quasi-linear chains, we finally estimated the number of molecules per chain as 3/5. This estimation is in a good agreement with the study of the hyper(hypo)chromism presented here. Similar estimations were also obtained in studies of the steady-state and the time-resolved spectra of *Cfx. aurantiacus* chlorosomes (Yakovlev et al. 2017, 2018). It should be noted that questions about how BChl chains are unified into 6-nm building blocks and how these blocks are further unified

Table 1 Estimation of the in vivo BChl *c* packing density for *Cfx. aurantiacus* chlorosomes (Staehelin et al. 1978; Golecki and Oelze 1987; Sprague et al. 1981)

	Low BChl <i>c</i> content culture	High BChl <i>c</i> content culture
Chlorosomal size, nm	12×34×96	19×38×108
Total number of molecules	~3400	~12,000
Number of rods	~12	~21
Number of molecules per rod	~280	~570
Number of units per rod	~16	~18
Number of molecules per unit	~18	~32
Number of molecules per chain	~3	~5

into rods still remain open due to the lack of conclusive information.

It is interesting to compare our theoretical results obtained in the framework of a rather simple model of J-/H-aggregates (Gülen 2006) with a more rigorous model based on the rod-like model of the tightly packed BChl *c/e* aggregates (Shibata et al. 2010). The model structure used by Shibata et al. (2010) was the same as it was originally proposed by Holzwarth and Schaffner (1994) and by Prokhorenko et al. (2000, 2003). The model of Shibata et al. (2010) showed that intensity borrowing between the Soret and Q_y bands significantly affects the absorption, linear dichroism, and circular dichroism spectra of *Chlorobaculum (Cba.) tepidum* (formerly *Chlorobium tepidum*) chlorosomes. This green sulfur bacterium has a very large chlorosomal antenna containing $\geq 10^5$ BChl molecules which is several times larger than the chlorosomal antenna size of *Cfx. aurantiacus* (Frigaard and Bryant 2006). This difference in the antenna size prevents a direct comparison of these two models. To obtain a good accordance with the experiment, it was additionally assumed by Shibata et al. (2010) that the B_x - and B_y -transition dipoles were not parallel to the molecular x- and y-axes, respectively. It was shown that in this case the optical spectra of chlorosomes are determined mainly by the local pigment arrangement of the aggregate, but not by its higher-order structure. Also, it was shown that the B_x band did not participate in the $B \rightarrow Q$ intensity borrowing in BChl *c* (but not in BChl *e*) aggregates. The calculated intensity borrowing from the B_y to the Q_y band in *Cba. tepidum* chlorosomes resulted in moderate Q_y -band hyperchromism and B_y -band hypochromism (Shibata et al. 2010).

It is widely accepted that the self-aggregation of chlorosomal BChls occurred by coordination of the 3^1 -hydroxy group of the molecule to the central Mg of another molecule and by the hydrogen bonding of the coordinated hydroxy group with the 13-keto carbonyl group of the third molecule (Smith et al. 1983; Krasnovsky and Bystrova 1980). Many types of ester groups including long straight chains are presented in the chlorosomal BChls (for review, see Tamiaki et al. 2007). These ester groups are suggested to participate in the formation of the higher-ordered structure of chlorosomes without any specific interaction with oligopeptides. For example, BChl *c* in *Cfx. aurantiacus* is esterified mainly with octadecanol (stearol). In chlorosomes, the ester groups of BChl molecules interact with flexible long chains of surrounding molecules. Chlorosomal BChl molecules have a long chain group at the 17-propionate ester which should interact with environmental molecules including the BChl molecules from the same or a neighboring rod, different molecules from the chlorosomal lipid sack (proteins, carotenoids and others), and the baseplate molecules. For example, the long chains of the molecules constituting the lipid monolayer directed to the chlorosomal interior and thus

interacted with the esterifying chains of aggregated BChls. This hydrophobic interaction would stabilize the relatively flexible lipid monolayer at the chlorosomal surface (Tamiaki et al. 2007). Therefore, the esterifying chains are important for the formation of a higher-ordered structure of chlorosomes which is important for efficient energy transfer in the chlorosomal self-aggregates.

Carotenoids play an important role in the chlorosome functioning mainly as photoprotectors. The nature of the interactions between BChls and carotenoids was studied by a combination of X-ray scattering, cryo-electron microscopy, absorption spectroscopy, and pigment analysis (Pšenčík et al. 2013). The data obtained by Pšenčík et al. (2013) were considered in favor of the lamellar structure of chlorosomes. *Cfx. aurantiacus* chlorosomes exhibit a carotenoid/BChl molar ratio in the range of 0.1–0.3. It was shown that *Cfx. aurantiacus* chlorosomes grown under higher light intensity contain more carotenoids, probably to provide more effective photoprotection (Pšenčík et al. 2013; Yakovlev et al. 2017). It was also shown that the lamellar spacing is roughly proportional to the length of BChl esterifying alcohols (Pšenčík et al. 2013). The length of these esterifying alcohols determines the lamellar spacing. The wider lamellae provide accumulation of a larger quantity of nonpolar molecules (such as carotenoids and quinones) in the hydrophobic region between the lamellar layers. The distance between the lamellar layers decreased when carotenoids were removed from the chlorosomes. A larger carotenoid content provides the effective photoprotection at a higher light intensity. It was suggested that *Cfx. aurantiacus* chlorosomal disorder is mainly due to the heterogeneity in the length of the esterifying alcohols and the larger amount of carotenoids (Pšenčík et al. 2013). The possible structural role of carotenoids needs to be further studied.

It should be noticed that the light-controlled variability of the building unit size during bacterial growth occurs not only in the peripheral BChl *c/d/e* chlorosomal antennae of green bacteria. For example, the structure of the peripheral BChl *a* antenna complex B-800 LH-2 of the purple photosynthetic bacterium *Rhodospseudomonas palustris* was shown to be also adapted to different light intensities during bacterial growth (Hartigan et al. 2002). The building unit of this peripheral antenna is composed of one B-800 monomer and one B-850 dimer. It was shown by X-ray crystallography that this building unit increased in size with decreasing light intensity during the culture growth (Hartigan et al. 2002). This change was accompanied by the aggregation of four exciton-coupled BChl *a* molecules.

Thus, the light intensity during bacterial growth controls both the size of the chlorosomal antenna of *Cfx. aurantiacus* and the size of its unit building block. As the light intensity decreases, the size of the peripheral antenna increases to enhance the light-absorbing capability and compensate

for the light deficit. The inevitable drop in the efficiency of light harvesting is accompanied by this increase in antenna size (Fetisova et al. 1996). This drop is compensated by an increase in the size of the unit building blocks that form the oligomeric BChl *c* aggregate. As a result of these structural changes, the high efficiency of light harvesting is maintained over a wide range of light intensities which allowed *Cfx. aurantiacus* to survive. An increase in the number of molecules per unit leads to a decrease in the total number of acts of energy transfer between units (if the total number of antenna molecules is fixed). This shortens the time of energy migration in the antenna and, consequently, provides less energy loss. If the total number of antenna molecules increases, then the number of units can be increased in the same proportion (the most favorable case) or in some smaller proportion, or remains the same (the most unfavorable case). In addition, an increase in the number of molecules per unit leads to an increase in the dipole strength of the Q_y absorption band, which enhances the absorption of light.

Conclusions

Here, we have demonstrated that Q-/B-band hyperchromism/hypochromism is an effective tool for studying the oligomeric structure of the *Cfx. aurantiacus* chlorosomes. We studied chlorosomes grown at different light intensities and, therefore, had different antenna sizes. We showed experimentally that Q-/B-bands hyperchromism/hypochromism is proportional to the size of the chlorosomal antenna. A theoretical explanation of these findings was based on the concept of excitonic intensity borrowing between the well-separated Q and B absorption bands. We used the model of J-/H-aggregates of BChls which predicted the dependence of Q-/B-bands hyperchromism/hypochromism on the structure of BChl aggregates (Gülen 2006). Being applied to exciton-coupled BChl *c* linear chains within the unit building block, the theory predicted an increase in the hyperchromism/hypochromism with an increase in the number of molecules per chain and a decrease in it with an increase in the number of chains. Comparison of experimental and theoretical results led to the conclusion that the unit building block of *Cfx. aurantiacus* chlorosomes comprises of several short BChl *c* chains. The number of BChl *c* molecules per chain varied from ~3 to ~5 depending on light intensity during culture growth. This conclusion is in accordance with previous linear and nonlinear spectroscopy studies on *Cfx. aurantiacus* chlorosomes. Thus, we demonstrated the light-controlled variability of the extent of BChl *c* aggregation within a unit building block in a variable peripheral antenna of *Cfx. aurantiacus* chlorosomes.

Control over the light-harvesting antenna size helps photosynthetic organisms to survive over a wide range of

light intensities. As the light intensity decreases, the size of the antenna increases to compensate for the light deficit by enhancing its light-absorbing capability. In general, this increase in the antenna size itself should be accompanied by a drop in the efficiency of the antenna functioning. However, Nature solve this problem in many ways, for example, by enlarging the size of the unit BChl aggregate to ensure high efficiency of energy transfer within the antenna. The primary processes of light energy harvesting in photosynthetic organisms are very efficient due to the structural optimization of their apparatus according to functional criteria (Fetisova and Fok 1984). One of the optimizing factors is the degree of oligomerization of antenna pigments (Fetisova et al. 1989) which is possible due to the self-aggregation of chlorophylls (Smith et al. 1983; Krasnovsky and Bystrova 1980). Self-organization of the ordered systems seems to be a key feature of all living systems.

Acknowledgements The authors are very grateful to Prof. Dr. Demet Gülen for fruitful cooperation and assistance in theoretical modeling. This work was supported in part by the Russian Foundation for Basic Research (Grants 18-04-00105a, 14-04-00295a).

Compliance with ethical standards

Conflict of interest The authors declare that they have no conflict of interest.

References

- Arellano J, Melo T, Borrego C, Garcia-Gil J, Naqvi K (2000) Nanosecond laser photolysis studies of chlorosomes and artificial aggregates containing bacteriochlorophyll *e*: evidence for the proximity of carotenoids and bacteriochlorophyll *a* in chlorosomes from *Chlorobium phaeobacteroides* strain CL1401. *Photochem Photobiol* 72:669–675
- Carbonera D, Bordignon E, Giacometti G, Agostini G, Vianelli A, Vannini C (2001) Fluorescence and absorption detected magnetic resonance of chlorosomes from green bacteria *Chlorobium tepidum* and *Chloroflexus aurantiacus*. A comparative study. *J Phys Chem B* 105:246–255
- Castenholz RW (1969) Thermophilic blue-green algae and the thermal environment. *Bacteriol Rev* 33:476–504
- Clayton RK (1980) *Photosynthesis: physical mechanisms and chemical patterns*. Cambridge University Press, Cambridge
- DeVoe H, Tinoco I Jr (1962) The hypochromism of helical polynucleotides. *J Mol Biol* 4:518–527
- Didraga C, Knoester J (2003) Absorption and dichroism spectra of cylindrical J aggregates and chlorosomes of green bacteria. *J Lumin* 102:60–66
- Dracheva T, Taisova A, Fetisova Z (1998) Circular dichroism spectroscopy as a test for the chlorosome antenna structure. In: Garab G (ed) *Photosynthesis: mechanisms and effects*, vol 1. Kluwer Academic Publishers, Dordrecht, pp 129–132
- Egawa A, Fujiwara T, Mizoguchi T, Kakitani Y, Koyama Y, Akutsu H (2007) Structure of the light-harvesting bacteriochlorophyll *c* assembly in chlorosomes from *Chlorobium limicola* determined by solid-state NMR. *Proc Natl Acad Sci USA* 104(3):790–795

- Fetisova Z (2004) Survival strategy of photosynthetic organisms. I. Variability of the extent of light-harvesting pigment aggregation as a structural factor optimizing the function of oligomeric photosynthetic antenna model calculations. *Mol Biol (Mosk)* 38:434–440
- Fetisova Z, Fok M (1984) Optimization routes for the transformation of light energy in primary acts of photosynthesis. I. The necessity of structure optimization for photosynthetic unit and method for the calculation of its efficiency. *Mol Biol (Mosk)* 18:1354–1359
- Fetisova Z, Kharchenko S, Abdourakhmanov I (1986) Strong orientational ordering of the near-infrared transition moment vectors of light-harvesting antenna bacterioviridin in chromatophores of the green photosynthetic bacterium *Chlorobium limicola*. *FEBS Lett* 199:234–236
- Fetisova Z, Freiberg A, Timpmann K (1988) Long-range molecular order as an efficient strategy for light harvesting in photosynthesis. *Nature (London)* 334:633–634
- Fetisova Z, Shibaeva L, Fok M (1989) Biological expedience of oligomerization of chlorophyllous pigments in natural photosynthetic systems. *J Theor Biol* 140:167–184
- Fetisova Z, Mauring K (1992) Experimental evidence of oligomeric organization of antenna bacteriochlorophyll *c* in green bacterium *Chloroflexus aurantiacus* by spectral hole burning. *FEBS Lett* 307:371–374
- Fetisova Z, Mauring K (1993) Spectral hole burning study of intact cells of green bacterium *Chlorobium limicola*. *FEBS Lett* 323:159–162
- Fetisova Z, Mauring K, Taisova A (1994) Strongly exciton coupled BChl *e* chromophore system in chlorosomal antenna of intact cells of green bacterium *Chlorobium phaeovibrioides*: A spectral hole burning study. *Photosynth Res* 41:205–210
- Fetisova Z, Freiberg A, Mauring K, Novoderezhkin V, Taisova A, Timpmann K (1996) Excitation energy transfer in chlorosomes of green bacteria: theoretical and experimental studies. *Biophys J* 71:101–995
- Frigaard N-U, Bryant DA (2004) Seeing green bacteria in a new light: genomics-enabled studies of the photosynthetic apparatus in green sulfur bacteria and filamentous anoxygenic phototrophic bacteria. *Arch Microbiol* 182:265–276
- Frigaard N-U, Bryant D (2006) Chlorosomes: antenna organelles in green photosynthetic bacteria. In: Shively JM (ed) *Complex intracellular structures in prokaryotes* Microbiology monographs, vol 2. Springer, Berlin, pp 79–114
- Furumaki S, Vacha F, Habuchi S, Tsukatani Y, Bryant D, Vacha M (2011) Absorption linear dichroism measured directly on a single light-harvesting system: the role of disorder in chlorosomes of green photosynthetic bacteria. *J Am Chem Soc* 133(17):6703–6710
- Furumaki S, Yabiku Y, Habuchi S, Tsukatani Y, Bryant D, Vacha M (2012) Circular dichroism measured on single chlorosomal light-harvesting complexes of green photosynthetic bacteria. *J Phys Chem Lett* 3:3545–3549
- Ganapathy S, Oostergetel G, Wawrzyniak P, Reus M, Gomez Maqueo Chew A, Buda F, Boekema E, Bryant D, Holzwarth A, de Groot H (2009) Alternating syn-anti bacteriochlorophylls form concentric helical nanotubes in chlorosomes. *Proc Natl Acad Sci USA* 106:8525–8530
- Gerola P, Olson J (1986) A new bacteriochlorophyll *a*-protein complex associated with chlorosomes of green sulfur bacteria. *Biochim Biophys Acta* 848:69–76
- Golecki J, Oelze J (1987) Quantitative relationship between bacteriochlorophyll content, cytoplasmic membrane structure and chlorosome size in *Chloroflexus aurantiacus*. *Arch Microbiol* 148:236–241
- Gomez Maqueo Chew A, Frigaard N-U, Bryant D (2007) Bacteriochlorophyllide *c* C-82 and C-121 methyltransferases are essential for adaptation to low light in *Chlorobaculum tepidum*. *J Bacteriol* 189(17):6176–6184
- Graczyk A, Żurek JM, Paterson MJ (2014) On the linear and non-linear electronic spectroscopy of chlorophylls: a computational study. *Photochem Photobiol Sci* 13:103–111
- Gülen D (2006) Significance of the excitonic intensity borrowing in the J-/H-aggregates of bacteriochlorophylls/chlorophylls. *Photosynth Res* 87:205–214
- Gunther L, Jendryny M, Bloemsmas E, Tank M, Oostergetel G, Bryant D, Knoester J, Köhler J (2016) Structure of light-harvesting aggregates in individual chlorosomes. *J Phys Chem B* 120:5367–5376
- Hartigan N, Tharia H, Sweeney F, Lawless A, Papiz M (2002) The 7.5-Å electron density and spectroscopic properties of a novel low-light B800 LH2 from *Rhodospseudomonas palustris*. *Biophys J* 82:963–977
- Holzwarth AR, Schaffner K (1994) On the structure of bacteriochlorophyll molecular aggregates in the chlorosomes of green bacteria. A molecular modelling study. *Photosynth Res* 41:225–233
- Jendryny M, Aartsma T, Köhler J (2014) Insights into the excitonic states of individual chlorosomes from *Chlorobaculum tepidum*. *Biophys J* 106:1921–1927
- Krasnovsky A, Bystrova M (1980) Self-assembly of chlorophyll aggregated structures. *BioSystems* 12:181–194
- Lin S, Van Amerongen H, Struve W (1991) Ultrafast pump-probe spectroscopy of bacteriochlorophyll *c* antennae in bacteriochlorophyll *a*-containing chlorosomes from the green photosynthetic bacterium *Chloroflexus aurantiacus*. *Biochim Biophys Acta* 1060:13–22
- Linnanto J, Korppi-Tommola J (2008) Investigation on chlorosomal antenna geometries: tube, lamella and spiral-type self-aggregates. *Photosynth Res* 96:227–245
- Linnanto J, Korppi-Tommola J (2013) Exciton description of chlorosome to baseplate excitation energy transfer in filamentous anoxygenic phototrophs and green sulfur bacteria. *J Phys Chem B* 117:11144–11161
- Ma Y-Z, Cox R, Gillbro T, Miller M (1996) Bacteriochlorophyll organization and energy transfer kinetics in chlorosomes from *Chloroflexus aurantiacus* depend on the light regime during growth. *Photosynth Res* 47:157–165
- Martiskainen J, Linnanto J, Kananavičius R, Lehtovuori V, Korppi-Tommola J (2009) Excitation energy transfer in isolated chlorosomes from *Chloroflexus aurantiacus*. *Chem Phys Lett* 477:216–220
- Martiskainen J, Linnanto J, Aumanen V, Myllyperkiö P, Korppi-Tommola J (2012) Excitation energy transfer in isolated chlorosomes from *Chlorobaculum tepidum* and *Prosthecochloris aestuarii*. *Photochem Photobiol* 88(3):675–683
- Mauring K, Novoderezhkin V, Taisova A, Fetisova Z (1999) Exciton levels structure of antenna bacteriochlorophyll *c* aggregates in the green bacterium *Chloroflexus aurantiacus* as probed by 1.8–293 K fluorescence spectroscopy. *FEBS Lett* 456:239–242
- Mimuro M, Hirota M, Nishimura Y, Moriyama T, Yamazaki I, Shimada K, Matsuura K (1994) Molecular organization of bacteriochlorophyll in chlorosomes of the green photosynthetic bacterium *Chloroflexus aurantiacus*: studies of fluorescence depolarization accompanied by energy transfer process. *Photosynth Res* 41:181–191
- Mirkovic T, Ostroumov E, Anna J, van Grondelle R, Govindjee SG (2017) Light absorption and energy transfer in the antenna complexes of photosynthetic organisms. *Chem Rev* 117(2):249–293
- Montaño G, Wu H, Lin S, Brune D, Blankenship R (2003) Isolation and characterization of the B798 light-harvesting baseplate from the chlorosomes of *Chloroflexus aurantiacus*. *Biochemistry* 42:10246–10251
- Novoderezhkin V, Taisova A, Fetisova Z, Blankenship R, Savikhin S, Buck D, Struve W (1998) Energy transfers in the B808–866

- antenna from the green bacterium *Chloroflexus aurantiacus*. *Biophys J* 74:2069–2075
- Novoderezhkin V, Taisova A, Fetisova Z (2001) Unit building block of the oligomeric chlorosomal antenna of the green photosynthetic bacterium *Chloroflexus aurantiacus*: modeling of nonlinear optical spectra. *Chem Phys Lett* 335:234–240
- Oelze J (1992) Light and oxygen regulation of the synthesis of bacteriochlorophyll *a* and bacteriochlorophyll *c* in *Chloroflexus aurantiacus*. *J Bacteriol* 174:5021–5026
- Oelze J, Golecki J (1995) Membranes and chlorosomes of green bacteria: structure, composition and development. In: Blankenship RE, Madigan MT, Bauer CE (eds) *Anoxygenic photosynthetic bacteria*. Kluwer Academic Publishers, Dordrecht, pp 259–278
- Olson JM (1980) Chlorophyll organization in green photosynthetic bacteria. *Biochim Biophys Acta* 594:33–51
- Olson J (1998) Chlorophyll organization and function in green photosynthetic bacteria. *Photochem Photobiol* 67:61–75
- Oostergetel G, van Amerongen H, Boekema E (2010) The chlorosome: a prototype for efficient light harvesting in photosynthesis. *Photosynth Res* 104(2–3):245–255
- Orf G, Blankenship R (2013) Chlorosome antenna complexes from green photosynthetic bacteria. *Photosynth Res* 116:315–331
- Pandit A, de Groot H (2012) Solid-state NMR applied to photosynthetic light-harvesting complexes. *Photosynth Res* 111:219–226
- Pierson B, Castenholz R (1974) Pigments and growth in *Chloroflexus aurantiacus*, a phototrophic filamentous bacterium. *Arch Microbiol* 100:283–305
- Pierson B, Castenholz R (1992) The family Chloroflexaceae. In: Balows A, Trüper H, Dworkin M, Harder W, Schleifer K (eds) *The prokaryotes*, vol 4, 2nd edn. Springer, Heidelberg, pp 3754–3774
- Pierson B, Castenholz R (1995) Taxonomy and physiology of filamentous anoxygenic phototrophs. In: Blankenship RE, Madigan MT, Bauer CE (eds) *Anoxygenic photosynthetic bacteria*. Kluwer Academic Publishers, Dordrecht, pp 31–47
- Prokhorenko VI, Steensgaard DB, Holzwarth AR (2000) Exciton dynamics in the chlorosomal antennae of the green bacteria *Chloroflexus aurantiacus* and *Chlorobium tepidum*. *Biophys J* 79:2105–2120
- Prokhorenko VI, Steensgaard DB, Holzwarth AR (2003) Exciton theory for supramolecular chlorosomal aggregates: 1. Aggregate size dependence of the linear spectra. *Biophys J* 85:3173–3186
- Pšenčík J, Ikonen T, Laurinmäki P, Merckel M, Butcher S, Serimaa R, Tuma R (2004) Lamellar organization of pigments in chlorosomes, the light harvesting system of green bacteria. *Biophys J* 87:1165–1172
- Pšenčík J, Torkkeli M, Zupčanová A, Vácha F, Serimaa R, Tuma R (2010) The lamellar spacing in self-assembling bacteriochlorophyll aggregates is proportional to the length of the esterifying alcohol. *Photosynth Res* 104:211–219
- Pšenčík J, Arellano J, Collins A, Laurinmäki P, Torkkeli M, Löflund B, Serimaa R, Blankenship R, Tuma R, Butcher S (2013) Structural and functional roles of carotenoids in chlorosomes. *J Bacteriol* 195:1727–1734
- Rich A, Tinoco I Jr (1960) The effect of chain length upon hypochromism in nucleic acids and polynucleotides. *J Am Chem Soc* 82:6409–6410
- Saga Y, Tamiaki H (2006) Transmission electron microscopic study on supramolecular nanostructures of bacteriochlorophyll self-aggregates in chlorosomes of green photosynthetic bacteria. *J Biosci Bioeng* 102:18–23
- Savikhin S, Zhu Y, Lin S, Blankenship RE, Struve WS (1994) Femtosecond spectroscopy of chlorosome antennas from the green photosynthetic bacterium *Chloroflexus aurantiacus*. *J Phys Chem* 98:10322–10334
- Savikhin S, Buck D, Struve W, Blankenship R, Taisova A, Novoderezhkin V, Fetisova Z (1998) Exciton delocalization in the bacteriochlorophyll *c* antenna of the green bacterium *Chloroflexus aurantiacus* as revealed by ultrafast pump-probe spectroscopy. *FEBS Lett* 430:323–326
- Sawaya N, Huh J, Fujita T, Saikin S, Aspuru-Guzik A (2015) Fast delocalization leads to robust long-range excitonic transfer in a large quantum chlorosome model. *Nano Lett* 15:1722–1729
- Scherz A, Parson WW (1984a) Oligomers of bacteriochlorophyll and bacteriophycocyanin with spectroscopic properties resembling those found in photosynthetic bacteria. *Biochim Biophys Acta* 766:653–665
- Scherz A, Parson WW (1984b) Exciton interactions in dimers of bacteriochlorophyll and related molecules. *Biochim Biophys Acta* 766:666–678
- Schmidt K, Maarzahl M, Mayer F (1980) Development and pigmentation of chlorosomes in *Chloroflexus aurantiacus* Ok-70-fl. *Arch Microbiol* 127:87–97
- Scholes GD, Fleming GR, Alexandra Olaya-Castro A, van Grondelle R (2011) Lessons from nature about solar light harvesting. *Nat Chem* 3:763–774
- Shibata Y, Saga Y, Tamiaki H, Itoh S (2006) Low temperature fluorescence from single chlorosomes, photosynthetic antenna complexes of green filamentous and sulfur bacteria. *Biophys J* 91:3787–3796
- Shibata Y, Saga Y, Tamiaki H, Itoh S (2007) Polarized fluorescence of aggregated bacteriochlorophyll *c* and baseplate bacteriochlorophyll *a* in single chlorosomes isolated from *Chloroflexus aurantiacus*. *Biochemistry* 46:7062–7068
- Shibata Y, Tateishi S, Nakabayashi S, Itoh S, Tamiaki H (2010) Intensity borrowing via excitonic couplings among Soret and Q_y transitions of bacteriochlorophylls in the pigment aggregates of chlorosomes, the light-harvesting antennae of green sulfur bacteria. *Biochemistry* 49:7504–7515
- Smith K, Kehres L, Fajer J (1983) Aggregation of bacteriochlorophylls *c*, *d* or *e*. Models for the antenna chlorophylls of green and brown photosynthetic bacteria. *J Am Chem Soc* 105:1387–1389
- Sprague S, Staehelin L, DiBartolomeis M, Fuller R (1981) Isolation and development of chlorosomes in the green bacterium *Chloroflexus aurantiacus*. *J Bacteriol* 147:1021–1031
- Staehelin L, Golecki J, Fuller R, Drews G (1978) Visualization of the supramolecular architecture of chlorosomes (*Chlorobium* type vesicles) in freeze-fractured cells of *Chloroflexus aurantiacus*. *Arch Microbiol* 119:269–277
- Taisova A, Gulen D, Iseri E, Drachev V, Cherenkova T, Fetisova Z (2001) Antenna-size dependent hyperchromism of the Q_y absorption band of chlorosomal oligomeric bacteriochlorophyll (BChl) *c* antennae of green bacteria. *Photosynth Res* 69:9
- Taisova A, Keppen O, Lukashev E, Arutyunyan A, Fetisova Z (2002) Study of the chlorosomal antenna of the green mesophilic filamentous bacterium *Oscillochloris trichoides*. *Photosynth Res* 74:73–85
- Taisova A, Keppen O, Novikov A, Naumova M, Fetisova Z (2006) Some factors controlling the biosynthesis of chlorosome antenna bacteriochlorophylls in green filamentous anoxygenic phototrophic bacteria of the family *Oscillochloridaceae*. *Microbiology* 75(2):129–135
- Tamiaki H (1996) Supramolecular structure in extramembraneous antennae of green photosynthetic bacteria. *Coord Chem Rev* 148:183–197
- Tamiaki H, Amakawa M, Holzwarth AR, Schaffner K (2002) Aggregation of synthetic metallochlorins in hexane. A model of chlorosomal bacteriochlorophyll self-assemblies in green bacteria. *Photosynth Res* 71:59–67
- Tamiaki H, Shibata R, Mizoguchi T (2007) The 17-propionate function of (bacterio)chlorophylls: biological implication of their long esterifying chains in photosynthetic systems. *Photochem Photobiol* 83:152–162

- Tinoco I (1960) Hypochromism in polynucleotides. *J Am Chem Soc* 82:4785–4790
- Tinoco I Jr (1962) Theoretical Aspects of Optical Activity. Part Two: Polymers *Advances in Chemical Physics*, vol 4, pp 113–160. Interscience Publishers, New York.
- Umetsu M, Wang ZY, Kobayashi M, Nozawa T (1999) Interaction of photosynthetic pigments with various organic solvents: magnetic circular dichroism approach and application to chlorosomes. *Biochim Biophys Acta* 1410:19–31
- Van Dorssen R, Amesz J (1988) Pigment organization and energy transfer in the green photosynthetic bacterium *Chloroflexus aurantiacus*. III. Energy transfer in whole cells. *Photosynth Res* 15:177–189
- Van Amerongen H, Vasmel H, van Grondelle R (1988) Linear dichroism of chlorosomes from *Chloroflexus aurantiacus* in compressed gels and electric fields. *Biophys J* 54:65–76
- Van Dorssen RJ, Vasmel H, Amesz J (1986) Pigment organization and energy transfer in the green photosynthetic bacterium *Chloroflexus aurantiacus* II. The chlorosome. *Photosynth Res* 9:33–45
- Yakovlev A, Novoderezhkin V, Taisova A, Fetisova Z (2002a) Exciton dynamics in the chlorosomal antenna of the green bacterium *Chloroflexus aurantiacus*: experimental and theoretical studies of femtosecond pump-probe spectra. *Photosynth Res* 71:19–32
- Yakovlev A, Taisova A, Fetisova Z (2002b) Light control over the size of an antenna unit building block as an efficient strategy for light harvesting in photosynthesis. *FEBS Lett* 512:129–132
- Yakovlev A, Taisova A, Arutyunyan A, Shuvalov V, Fetisova Z (2017) Variability of aggregation extent of light-harvesting pigments in peripheral antenna of *Chloroflexus aurantiacus*. *Photosynth Res* 133:343–356
- Yakovlev AG, Taisova AS, Shuvalov VA, Fetisova ZG (2018) Estimation of the bacteriochlorophyll *c* oligomerisation extent in *Chloroflexus aurantiacus* chlorosomes by very low-frequency vibrations of the pigment molecules: a new approach. *Biophys Chem* 240:1–8

Publisher's Note Springer Nature remains neutral with regard to jurisdictional claims in published maps and institutional affiliations.